

Electronic Supplementary Information

Binding TiO₂-B nanosheets with N-doped carbon enables highly durable anodes for lithium-ion batteries

Chaoji Chen,^a Bao Zhang,^b Ling Miao,^b Mengyu Yan,^c Liqiang Mai,^c Yunhui

Huang^{*a} and Xianluo Hu^{*a}

^a State Key Laboratory of Materials Processing and Die & Mould Technology, School of Materials Science and Engineering, Huazhong University of Science and Technology, Wuhan 430074, China

^b Wuhan National Laboratory for Optoelectronics, and School of Optical and Electronic Information, Huazhong University of Science and Technology, Wuhan 430074, China

^c State Key Laboratory of Advanced Technology for Materials Synthesis and Processing, Wuhan University of Technology, Wuhan 430070, China

*Correspondence to: huxl@mail.hust.edu.cn; huangyh@hust.edu.cn

Supplementary Method S1: calculation details for the separation of the diffusion- and capacitive-controlled charge

Generally, the total current (or charge) of the electrode at a certain potential comprises two components, described by the equation of $i(V) = k_1v^{1/2} + k_2v$ and $i(V)/v^{1/2} = k_1 + k_2v^{1/2}$ (Eq. 1), based on the power law relationship of $i = av^{1/2}$ for the diffusion-controlled processes and $i = av$ for the capacitive-controlled processes. From the cyclic voltammograms at various scan rates of 0.1–2 mV s⁻¹, the current values can be determined when the voltage is given. According to Eq. 1, the values of k_1 (intercept) and k_2 (slope) at a fixed potential can be determined by plotting curves of $i(V)/v^{1/2}$ vs. $v^{1/2}$ (v varies from 0.1 to 2 mV s⁻¹). When k_1 and k_2 values at each voltage are quantified, the values of $k_1v^{1/2}$ and k_2v at a certain scan rate (v) can be determined, thus the diffusion-controlled current ($k_1v^{1/2}$) and capacitive-controlled current (k_2v) be separated.

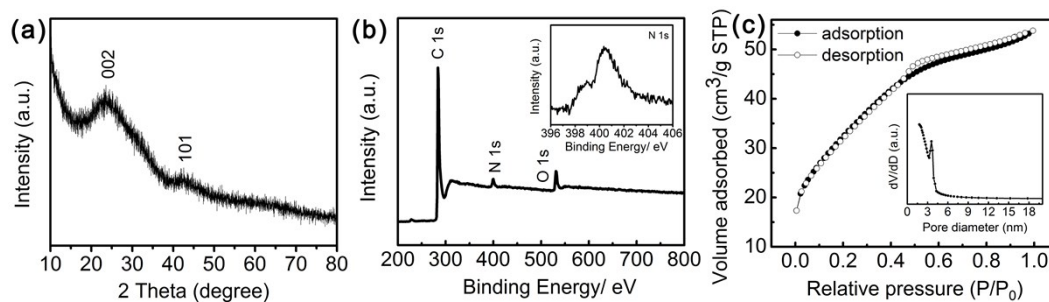


Fig. S1 Structure characterizations of NPC: (a) XRD pattern, (b) survey XPS spectrum, inset is the high-resolution XPS N 1s spectrum and (c) nitrogen adsorption/desorption isotherms, inset is the pore-size distribution. All peaks in the XRD pattern can be indexed to hard carbon. The survey XPS spectrum shows three peaks of C 1s, N 1s and O1s, indicating the existence of doping N in the NPC material, which can be further confirmed by the high-resolution XPS N 1s spectrum. The NPC demonstrates a meso- and microporous structure with a large BET surface area of $2611 \text{ m}^2 \text{ g}^{-1}$.

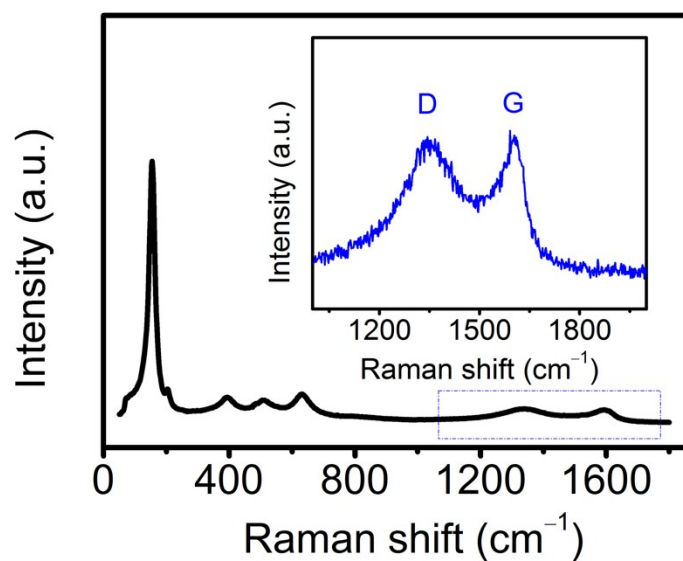


Fig. S2 Raman spectrum for the NPC-TiO₂-B hybrid.

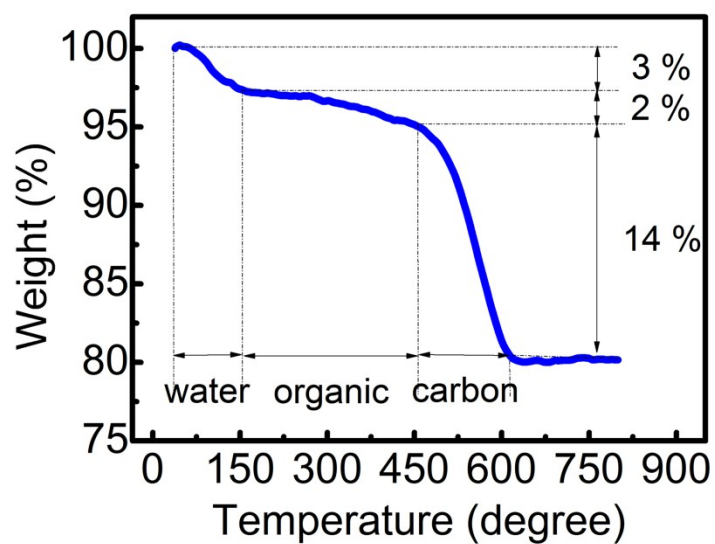


Fig. S3 TG curve for the precursor of the NPC-TiO₂-B hybrid. Accordingly the carbon content in the NPC- TiO₂-B hybrid is about 14 wt.%.

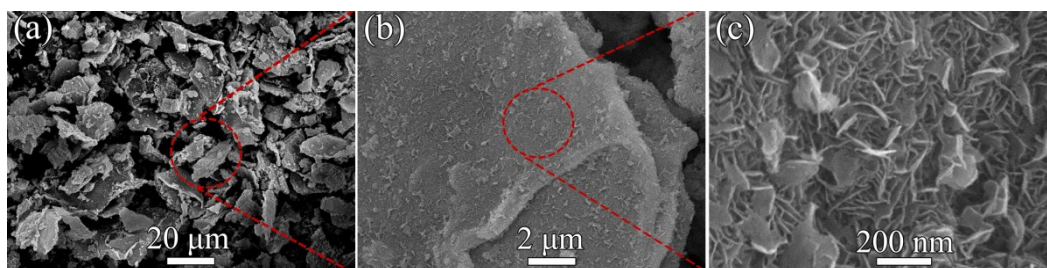


Fig. S4 (a-c) SEM images of the NPC-TiO₂-B hybrid. Numerous nanosheets grow inside and outside the carbon skeleton, forming a bulky hybrid architecture of dozens of micrometers in width and length.

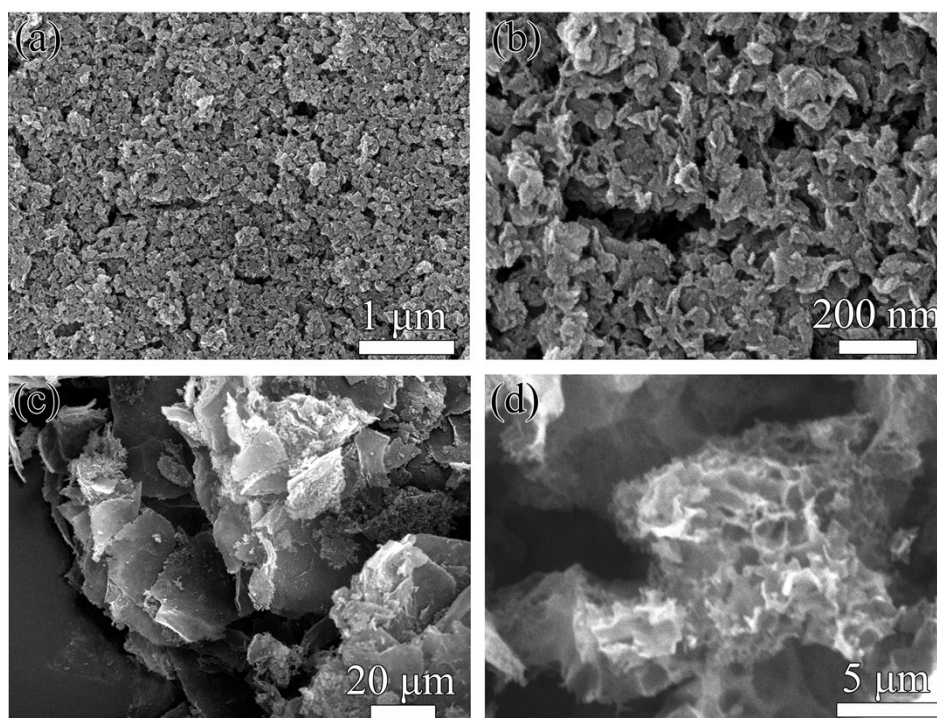


Fig. S5 SEM images of TNS (a,b) and NPC (c,d).

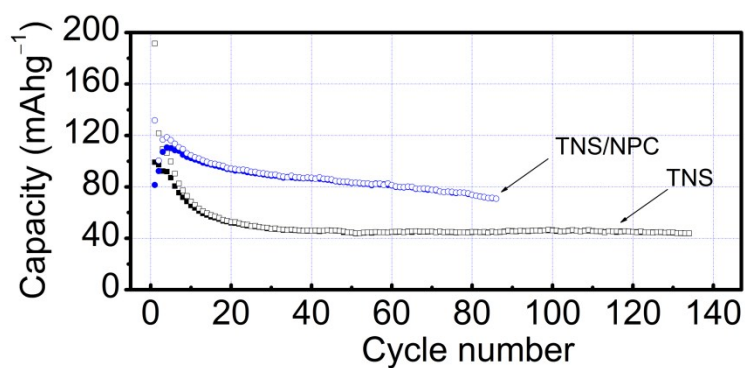


Fig. S6 Electrochemical lithium-storage performance of the TNS and TNS/NPC electrodes: discharging-charging at a current density of 500 mA g⁻¹.

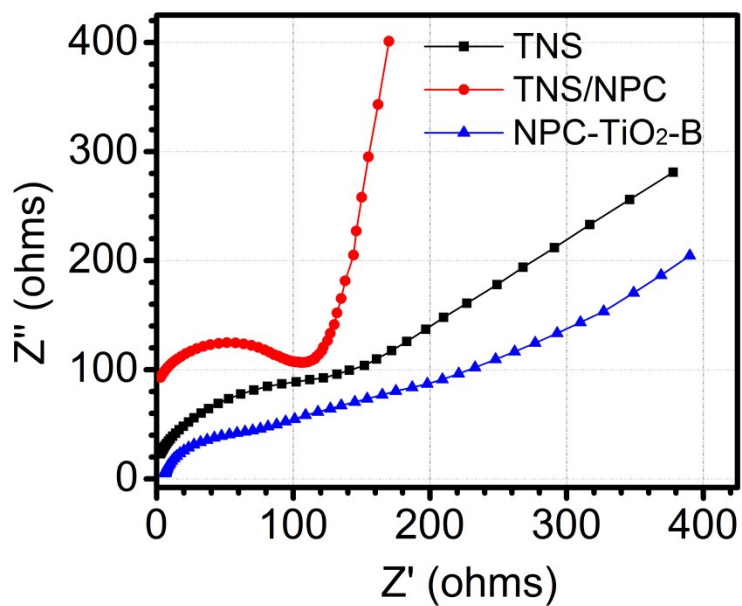


Fig. S7 EIS spectra for the three electrodes after 1 discharge-charge cycle.

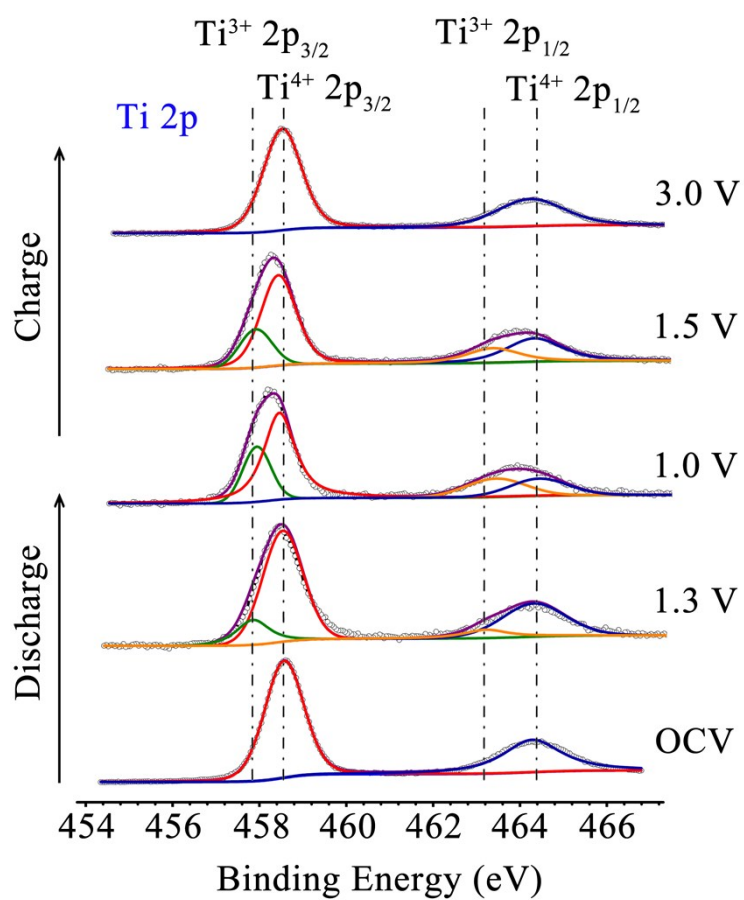


Fig. S8 Ex-situ high-resolution XPS spectra of Ti 2p for the NPC-TiO₂-B electrodes at various states of discharge then charge.